

Minimal conductivity, topological Berry winding and duality in three-band semimetals

Thibaud Louvet, Pierre Delplace, Andrei A. Fedorenko, and David Carpentier
Laboratoire de Physique, École Normale Supérieure de Lyon, 47 allée d'Italie, 69007 Lyon, France
(Dated: March 13, 2015)

The physics of massless relativistic quantum particles has recently arisen in the electronic properties of solids following the discovery of graphene. Around the accidental crossing of two energy bands, the electronic excitations are described by a Weyl equation initially derived for ultra-relativistic particles. Similar three and four band semimetals have recently been discovered in two and three dimensions. Among the remarkable features of graphene are the characterization of the band crossings by a topological Berry winding, leading to an anomalous quantum Hall effect, and a finite minimal conductivity at the band crossing while the electronic density vanishes. Here we show that these two properties are intimately related: this result paves the way to a direct measure of the topological nature of a semi-metal. By considering three band semimetals with a flat band in two dimensions, we find that only few of them support a topological Berry phase. The same semimetals are the only ones displaying a non vanishing minimal conductivity at the band crossing. The existence of both a minimal conductivity and a topological robustness originates from properties of the underlying lattice, which are encoded not by a symmetry of their Bloch Hamiltonian, but by a duality.

Electronic excitations which satisfy ultra relativistic quantum physics emerge around the band crossing of semimetals. While graphene constitutes the canonical example of such a phase, the discovery of topological insulators opened the route to other realizations [1]: such semimetals exist at the transitions between topological and trivial insulators. Theoretical proposals were initiated by the identification of crystalline symmetries stabilizing these critical phases both in two and three dimensions [2]. This idea turned out to be particularly successful: recently, a Weyl semimetal corresponding to two band crossings in three spatial dimensions was discovered in TaAs [3, 4]. The existence of a three band crossing semimetal was proposed in a two dimensional carbon allotrope SG-10b [5] and square MoS₂ sheet [6], and discovered in three dimensions in HgCdTe [7]. Stable four band crossing semimetals in three dimensions, denoted Dirac phases, were proposed theoretically and experimentally identified in Na₃Bi [4, 8, 9] and in Cd₃As₂ [10–12], and predicted in β -cristobalite BiO₂ [2] and distorted spinels [13].

In the case of graphene, the relativistic nature of the electronic excitations translates into remarkable transport properties including an anomalous half-integer Hall

effect with half integer plateaus and a non vanishing minimal conductivity exactly at the band crossing [14–17]. The anomalous half-integer Hall effect is related to the topological properties of the band crossing: when winding around the crossing point, an electron picks up a quantized so-called Berry phase. This Berry phase is at the origin of the half-integer nature of the quantum Hall effect in graphene [15, 18], but also characterizes the topological property of the semi-metallic phase encoding its robustness towards gap opening perturbations [1]. On the other hand the minimal conductivity at the band crossing was associated to the Zitterbewegung of Dirac particles, an intrinsic agitation characteristic of ultra relativistic particles which leads to diffusive motion even in perfectly clean samples [16, 19].

In this article we consider these characteristic signatures of semimetals beyond the two-band crossing situation of graphene. When a third locally flat band is present at the crossing, none of these properties is necessarily enforced. Indeed, we find that the exact same models possess both a non vanishing minimal conductivity and a topological Berry winding at the crossing. Hence these properties are not hallmarks of a relativistic energy spectrum: they encode phase properties of the electronic wave functions. In the case of graphene, this phase winding originates from the hexagonal lattice of carbon atoms. We will show that the lattice properties at the origin of these remarkable transport signatures are encoded not by a standard symmetry constraints of Bloch Hamiltonians, but by a duality transformation. We identify two duality classes, corresponding to the two signatures: the existence or not of both a non-vanishing minimal conductivity and a topological Berry winding.

Chirality or sublattice symmetry. We consider three-band semimetals in two dimensions characterized by two linearly crossing energy bands $n = \pm$ and a third locally flat band $n = 0$, represented in Fig. 1. This corresponds to the situation of HgCdTe in three dimensions [7], or the carbon allotrope SG-10b [5] and square MoS₂ sheet [6] in two dimensions. The energy spectrum $E(\vec{k})$ as a function of the momentum \vec{k} exhibits the symmetry $E(\vec{k}) \rightarrow -E(\vec{k})$ at least locally around the crossing point. This spectrum symmetry naturally originates from a chiral symmetry of the corresponding (low energy) Hamiltonian. This symmetry is represented by a unitary operator C that *anticommutes* with the Hamiltonian: $\mathcal{H} = -CHC$.

An explicit chiral operator can be defined when considering the pedagogical examples of tight-binding Hamiltonians defined on lattices. Similarly to graphene, only

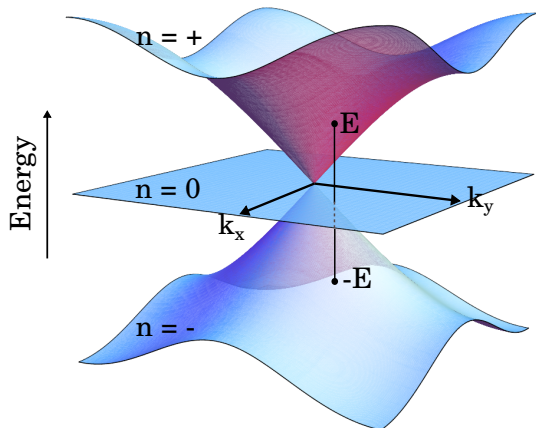


FIG. 1: Energy spectrum of a three-band chiral semimetal which shows a symmetry $E(\vec{k}) \rightarrow -E(\vec{k})$. Such a spectrum consists of two linear energy bands $n = \pm$ and a flat band $n = 0$.

nearest neighbor couplings can be kept when focusing around the band crossing points. In this case chiral symmetry corresponds to a sub-lattice symmetry: couplings are only present between the two sub-lattices A and B of a bipartite lattice. This is the case of the nearest neighbor description of graphene on the honeycomb lattice. In the case we consider in this article, three bands crossing implies the existence of three orbitals distributed on three Bravais lattices A_1, A_2 and B of same geometry, as shown on Fig. 2. Chiral symmetry is satisfied if the only couplings t_1, t_2 relevant at low energy are between orbitals on the B and the A_1, A_2 lattices whereas A_1 and A_2 stay uncoupled. The corresponding Bloch Hamiltonian in the orbital basis (A_1, A_2, B) is written

$$H(t_1, t_2; \vec{k}) = \begin{pmatrix} 0 & 0 & t_1 f_1(\vec{k}) \\ 0 & 0 & t_2 f_2(\vec{k}) \\ t_1 f_1^*(\vec{k}) & t_2 f_2^*(\vec{k}) & 0 \end{pmatrix}. \quad (1)$$

Such a Hamiltonian anti-commutes with a chirality operator $C = \text{diag}(1, 1, -1)$. The complex functions $f_j(\vec{k}) = |f_j(\vec{k})|e^{i\phi_j(\vec{k})}$ encode the geometry of the lattice of couplings. Their amplitudes determine the spectrum of the semimetal: $E_0(\vec{k}) = 0, E_{\pm}(\vec{k}) = \pm(t_1^2|f_1(\vec{k})|^2 + t_2^2|f_2(\vec{k})|^2)^{\frac{1}{2}}$. A three band crossing occurs when f_1 and f_2 vanish simultaneously at a point \vec{K} in the Brillouin zone. In this article, we focus on properties which depend on the phases $\phi_j(\vec{k})$ and which are thus *independent* of the spectrum provided a band crossing occurs.

Quite generally, we will consider chiral symmetric Bloch Hamiltonians describing a three-band semimetal with band crossing at point \vec{K} , and whose linear expan-

sion around the crossing takes the form

$$H(\vec{K} + \vec{q}) = \begin{pmatrix} 0 & 0 & \Lambda_{11}q_x + \Lambda_{12}q_y \\ 0 & 0 & \Lambda_{21}q_x + \Lambda_{22}q_y \\ \Lambda_{11}^*q_x + \Lambda_{12}^*q_y & \Lambda_{21}^*q_x + \Lambda_{22}^*q_y & 0 \end{pmatrix}. \quad (2)$$

Such a Hamiltonian is entirely parametrized by a matrix $\Lambda = \{\Lambda_{ij}\}$ of complex coefficients. The phase of the coefficients Λ_{ij} encodes the geometry of the underlying lattice. The corresponding geometrical constraint on these phases must be independent of the amplitude of couplings between the orbitals. Hence it cannot result in a symmetry of the Hamiltonian: we show that it corresponds to a duality in a manner analogous to the Kramers-Wannier duality of statistical mechanics models which relates models with different coupling amplitudes on different lattices [20].

Lattice geometry and duality constraints. The geometry of the lattice can be described by two vectors \vec{e}_1 and \vec{e}_2 relating a vector of the lattice B to neighbor sites of the A_1 and A_2 lattices, as shown on figure 2. The duality transformation \mathcal{D} exchanges the lattices A_1 and A_2 , or equivalently the vectors \vec{e}_1 and \vec{e}_2 , while simultaneously exchanging the couplings between B and A_1 orbitals with couplings between B and A_2 orbitals. Quite generally, this duality which is an involutive transformation *i.e.* $\mathcal{D}^2 = \mathbf{I}$, relates a Hamiltonian \mathcal{H} on a lattice \mathcal{L} to a Hamiltonian $\tilde{\mathcal{H}}$ on a *different* lattice $\tilde{\mathcal{L}}$. However, on symmetric lattices where initial and dual lattices $\mathcal{L}, \tilde{\mathcal{L}}$ are related by a geometrical transformation \mathcal{R} , this duality translates into constraints on Hamiltonians defined on the same lattice (or same Hilbert space). In this case, and focusing for simplicity on nearest neighbor Hamiltonians, the duality transformation can be recast into the form

$$(DU)H(t_2, t_1; \mathcal{R}\vec{k})(DU)^{-1} = H(t_1, t_2; \vec{k}) \quad (3)$$

where U is a unitary operator, \mathcal{R} is the symmetry relating initial and dual lattices and D the operator swapping A_1 and A_2 orbitals:

$$D = \begin{pmatrix} 0 & 1 & 0 \\ 1 & 0 & 0 \\ 0 & 0 & 1 \end{pmatrix}. \quad (4)$$

A very special case, which we call the duality class \mathcal{D}_I corresponds to the situation where two orbitals lie on the same geometrical lattice, *i.e.* when $\vec{e}_1 = \vec{e}_2 \neq \vec{0}$. In this class, the duality transformation simplifies and U and \mathcal{R} reduce to the identity. In this case, Bloch Hamiltonians encode the geometrical properties of a bipartite lattice, whereas in the other case, which we denote the duality class \mathcal{D}_{II} , the underlying lattices are either Bravais lattices or possess three distinct sublattices. This duality restricts the form of the chiral tight-binding Hamiltonian

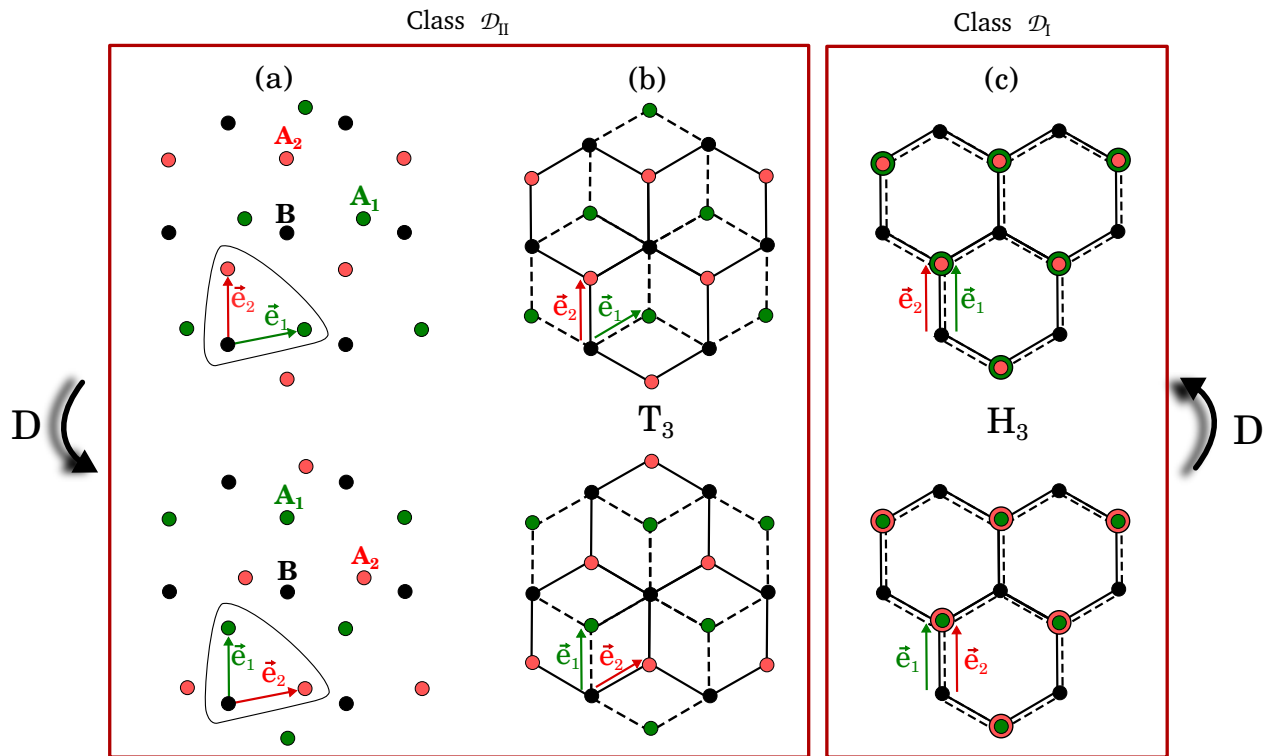


FIG. 2: Triangular Bravais lattices with three orbitals (A_1 , A_2 and B) per unit cell. The position of the A_1 orbitals is chosen arbitrary (a), in the center of the BA_1 hexagons (b), or at the same location than the A_2 orbitals (c) The duality transformation \mathcal{D} exchanges the location of the orbitals A_1 and A_2 and the hopping amplitudes symbolized by full/dashed lines. The original T_3 lattice is recovered after an inversion in (b) whereas the dual and the original lattices coincide for the H_3 lattice in (c).

(1): in the class \mathcal{D}_I we have $f_1(\vec{k}) = f_2(\vec{k})$ while a much weaker constrain $f_1(\vec{k}) = f_2(\mathcal{R}\vec{k})$ holds in class \mathcal{D}_{II} for symmetric lattices. Generalizing this constrain to a local Bloch Hamiltonian (2) around a three band crossing, the duality in class \mathcal{D}_I implies the condition

$$\frac{\Lambda_{21}}{\Lambda_{11}} = \frac{\Lambda_{22}}{\Lambda_{12}} \equiv \lambda, \quad (5)$$

while generically it only relates Hamiltonian at different crossing points in class \mathcal{D}_{II} . In the following we show that Hamiltonians belonging to the duality class \mathcal{D}_I describe the only three-band semimetals possessing quantized topological Berry windings which are also those whose conductivity does not vanish at the band crossing and display a pseudo-diffusive regime.

To illustrate this relation, let us discuss two nearest-neighbor lattice models of semi-metals belonging to both classes. A natural model in class \mathcal{D}_I , inspired by graphene, corresponds to a honeycomb lattice with two orbitals on one of the two sub-lattices, shown on Fig. 2 (c). The three bands of this model, which we call H_3 , cross at points \vec{K} and \vec{K}' of the Brillouin zone. Around those points, the Bloch Hamiltonian takes the

form (2) with a matrix of coefficients

$$\Lambda_{H_3} = \frac{3a}{2} \begin{pmatrix} t_1 & -it_1 \\ t_2 & -it_2 \end{pmatrix}, \quad (6)$$

with a being the honeycomb lattice spacing, while the characteristic energy scale of nearest neighbor couplings is encoded into $t = \sqrt{t_1^2 + t_2^2}$. This model satisfies the condition (5) with $\lambda = -i$ and belongs to the duality class \mathcal{D}_I . The T_3 model [21] is again defined on a honeycomb lattice but with additional orbitals A_2 at the center of each hexagon as shown on Fig. 2 (b). These orbitals are coupled by an amplitude t_2 only to the B sub-lattice of the honeycomb lattice, while A_1 and B orbitals on the honeycomb lattices are coupled by t_1 . This model belongs to the duality class \mathcal{D}_{II} , with the inversion $\mathcal{R}\vec{k} = -\vec{k}$ relating initial and dual lattices. Indeed, the Bloch Hamiltonian linearized around the band touching point \vec{K} is written in the form (2) with

$$\Lambda_{T_3} = \frac{3a}{2} \begin{pmatrix} t_1 & -it_1 \\ t_2 & it_2 \end{pmatrix}, \quad (7)$$

which does not fulfill the condition (5). Note that when $t_1 = t_2$, this linearized Hamiltonian can be written in the form $H_{\mathbf{K}}(\mathbf{q}) = \hbar v_F \mathbf{S} \cdot \mathbf{q}$, where S_x , S_y and $S_z \equiv$

diag(1, -1, 0) satisfy the spin-1 algebra $[S_i, S_j] = i\epsilon_{ijk}S_k$. Hence the T_3 model realizes a continuous deformation of spin-1 massless fermions, which all belong to the duality class \mathcal{D}_{II} .

We now characterize both the topological properties of the band crossing, as well as the electronic transport properties around the crossing, which turn out to be associated to the duality class of the semi-metal.

Topological property of a band crossing. The topological properties of band crossings in two dimensional crystals can be described by a topological invariant associated to each band around the crossing point. These invariants are the Berry phases γ_n (see eq.(10) of Methods) acquired by Bloch eigenstates Ψ_n upon winding around the crossing point \vec{K} . By definition this Berry winding is independent of the path winding around the crossing point: it is an homotopy invariant of a given Hamiltonian. It describes a *topological* property of the semimetal when it is robust against perturbations of the Hamiltonian which do not lift the band crossing. Such a robustness occurs when this Berry winding is quantized. This is indeed the case in graphene where $\gamma_{\pm} = \pm 1$. For the three-bands semi-metals, these Berry windings can be readily obtained from the diagonalisation of the Hamiltonian (2). We find that these windings are topological only when the condition (5) is fulfilled: the only semimetals characterized by a topological Berry winding are those of the duality class \mathcal{D}_I , with values

$$\gamma_+ = \gamma_- = \text{sgn Im } \lambda \quad , \quad \gamma_0 = -2 \text{sgn Im } \lambda \quad . \quad (8)$$

These quantized values of the Berry windings are stable with respect to any perturbation compatible with the duality constraint, *i.e.* which does not break the geometry of the underlying lattice. Eigenstates of the H_3 model (6) are characterized by Berry phases $\gamma_{\pm} = -1$, $\gamma_0 = 2$ as shown in Fig. 3. These windings are in particular robust to variations of hopping amplitudes t_1, t_2 . For any chiral symmetric semimetal which does not belong to the \mathcal{D}_I class, the Berry phase can take any real value and depends continuously on deformations of the Hamiltonian. This result is illustrated for the T_3 model (7) in Fig. 3: the Berry phases γ_n are shown to vary continuously upon variation of the ratio t_2/t_1 of nearest neighbor couplings.

Minimal conductivity at the band crossing. Transport measurements constitute a powerful tool to probe the physical properties in the vicinity of the Fermi energy. We will show that close to the band crossing electronic transport is related to the phase content of the Hamiltonian (the phases $\phi_i(\vec{k})$ of the amplitudes in (1)) and not to the spectrum. Remarkably, in graphene, when the Fermi level coincides with the twofold band crossing point, the conductivity of a clean sample was predicted to remain finite despite a vanishing density of states. This result was first derived by considering the conductivity of a narrow strip of graphene between two contact electrodes as shown on Fig. 4. Let us consider an analogous setup for a three band chiral semimetal, *i.e.*

a finite sample of length L and width W . Confinement of the sample between the leads gives rise to zero-energy evanescent states. At the band crossing, the conductivity depends entirely on the nature of these evanescent states. Prior to an explicit calculation of the conductivity (see Methods), it is instructive to consider the current operator $j_x(\vec{k}) = \langle \partial_{k_x} H(\vec{k}) \rangle_{\psi}$ defined from the tight-binding Bloch Hamiltonian (1). Introducing the amplitudes $(\psi_{A_1}, \psi_{A_2}, \psi_B)$ of the electronic wavefunction in the three sub-lattices the longitudinal current can be expressed as $j_x(\vec{k}) = 2 \text{Re}[\psi_B(\vec{k})(\partial_{k_x} f_i(\vec{k})\psi_{A_i}^*(\vec{k}))]$ and is found to be proportional to the amplitude ψ_B on the B sub-lattice [23]. This hints that electronic transport at the band crossing will occur provided the zero-energy evanescent modes have a non-vanishing component on the B sub-lattice.

As expected from the previous qualitative argument, the existence of a finite minimal conductivity at the threefold band crossing point is uniquely determined by the non vanishing weight of the wave function on the hub lattice as we have checked using a Landauer description of transport (see Methods). From (2), this component is found to satisfy

$$\Lambda \cdot \begin{pmatrix} q_x \\ q_y \end{pmatrix} \psi_B = 0 \quad . \quad (9)$$

Hence the condition of existence of a non-vanishing minimal conductivity at the band crossing is simply $\det \Lambda = 0$. This constraint exactly coincides with the duality constraint (5) defining the class \mathcal{D}_I : the only three band semi-metals with a non-vanishing minimal conductivity are exactly those belonging to this duality class \mathcal{D}_I . Moreover for the H_3 lattice model, this minimal conductivity corresponds exactly to the value $\sigma^{(\text{min})} = e^2/(\pi h)$ predicted for graphene. This result remains valid for any model in the dual class \mathcal{D}_I with an isotropic dispersion relation. For more general three band semi-metals with an anisotropic dispersion relation, the minimal conductivity depends on the angle between the leads and the principal axes of the dispersion relation. However, the determinant of the corresponding conductivity tensor remains constant given by its isotropic value $\det \bar{\sigma} = (e^2/(\pi h))^2$. In contrast, any three-band chiral symmetric semimetal that does not belong to the \mathcal{D}_I class possesses a vanishing conductivity $\sigma^{(\text{min})} = 0$ in every directions. Beyond the minimal conductivity, the fluctuations of this conductivity can also be considered : their amplitude is encoded in the ratio between the shot noise power and the averaged current, the so-called Fano factor. This factor F takes a constant value $F = 1/3$ within the duality class \mathcal{D}_I , a value already encountered in graphene [16] and characteristic of diffusive metals [24]. Such a result demonstrates that for all semi-metals in this class the transport through narrow perfectly clean junctions displays the characteristic features of diffusive metals.

We have evaluated the conductivity of different lattice models in the geometry of Fig. 4. We compare the analytical results to a numerical Landauer approach (see

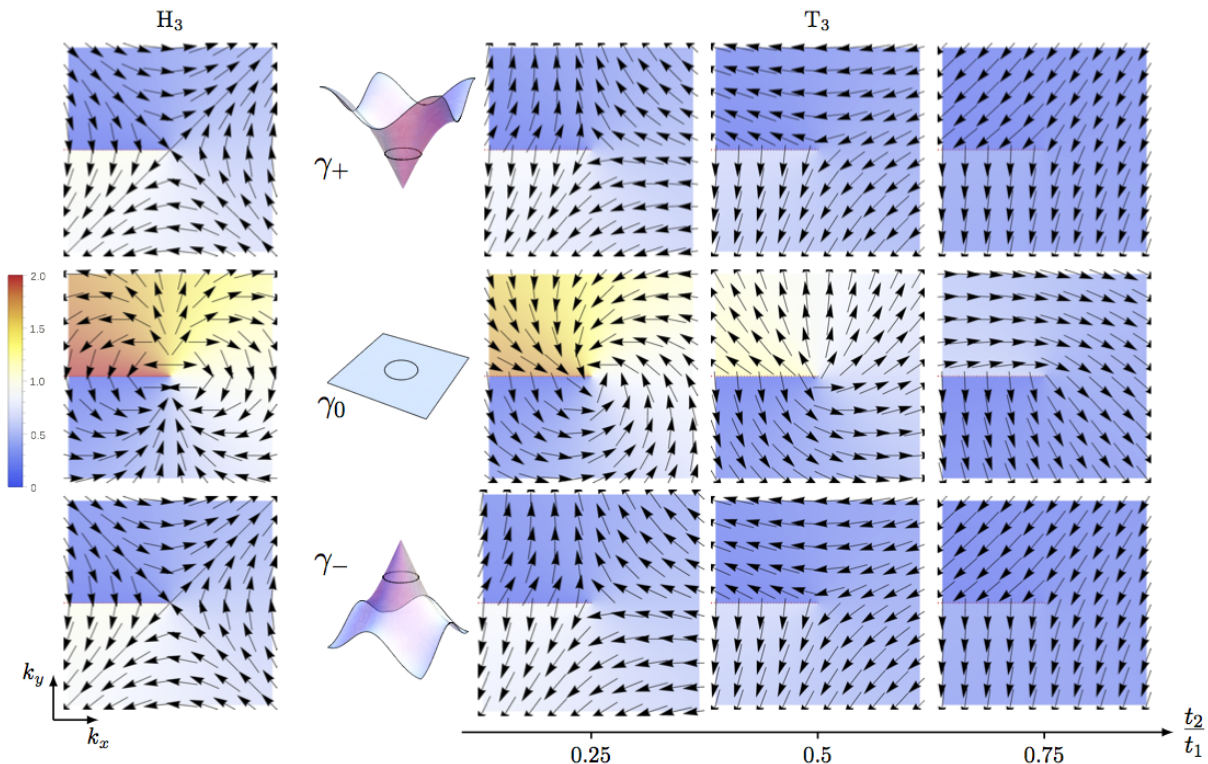


FIG. 3: Momentum dependence of the phase associated with the Berry connection for the three energy levels $n = -, 0, +$ for nearest neighbors models on the H_3 and on the T_3 model for three different values of the ratio of couplings between sub-lattices. A vortex is associated with a π Berry phase. For the H_3 lattice model, the Berry phase γ_n (10) along any closed loop winding around the origin is quantized (in units of π) and signals a topological property of the band crossing points. This is not the case for the T_3 lattice model, where this Berry phase continuously decreases and vanishes as a function of the couplings.

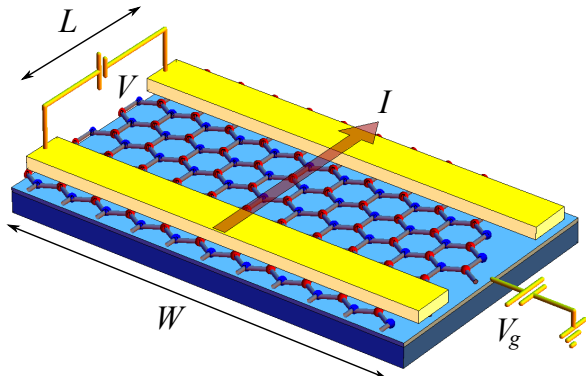


FIG. 4: The setup for two-terminal transport measurements: a 2D sample of size $W \times L$ with leads attached on opposite sides.

Methods) to check for possible inter-crossing point effects, neglected in the analytical approach. A perfect agreement is found between both approaches. The results for the H_3 model are shown as a function of the

Fermi-energy, or gate potential V_g on Fig. 5a: the conductivity exhibits a plateau around the band crossing point $V_g = 0$, corresponding to $\sigma = e^2/(\pi h)$. The results of a similar study for the T_3 model are also shown on Fig. 5a and display a collapse of the conductivity around the band crossing point $V_g = 0$ for three different values of the couplings between orbitals (Inset). Fig. 5b displays the analytical results for the dependance of the Fano factor on the gate potential V_g . We show that for the T_3 model $F(V_g = 0) = 1$, whereas for the H_3 model the Fano factor reaches the value $F = \frac{1}{3}$ at the band crossing, characteristic of a disordered metal as expected for class \mathcal{D}_1 . Finally, let us mention that for graphene the result of the Landauer formula for a narrow junction can be recovered for a long junction by an approach based on the Kubo formula [25]. While this equivalence remains valid for three band semimetals in the dual class \mathcal{D}_1 , it does not hold beyond it: we found that the Kubo conductivity for the T_3 model diverges at the band crossing, as opposed to the vanishing Landauer conductivity for a narrow junction, in agreement with a previous result in the disordered limit [26].

As follows from our results, the occurrence of a transport regime with a non vanishing conductivity at the

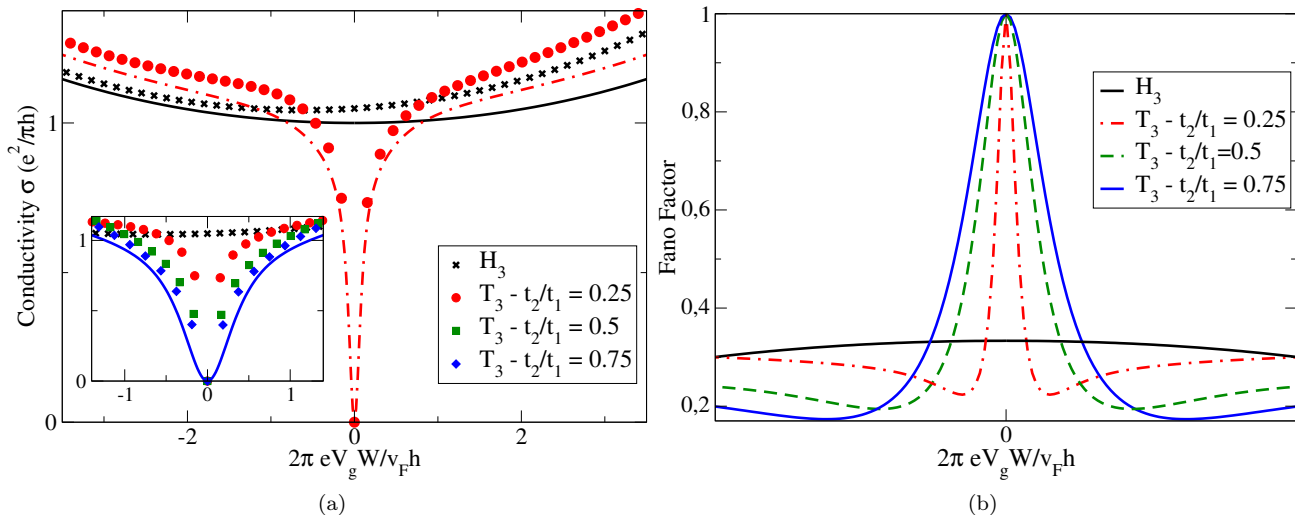


FIG. 5: Conductivity (a) and Fano factor (b) as a function of a gate potential V_g applied to the sample of size $L = 100, W = 300$ in units of lattice spacing a . Fermi velocity is given by $v_F = 3at/(2\hbar)$. Results for nearest neighbor lattices models on the H_3 and T_3 lattices are shown for various ratio t_2/t_1 of couplings between the different lattices.

crossing is not a generic property of linear dispersion relations near this crossing, nor a hallmark of relativistic physics of the associated electronic excitations such as the Zitterbewegung. It is indeed intimately related to the existence of a topological robustness of this band crossing, originating from lattice-properties encoded into the class \mathcal{D}_1 condition. This result opens the route to a direct probe of topological properties of semimetals through transport measurements around the band crossing. In graphene, a quantitative measurement of the conductivity exactly at the band crossing is hampered by fluctuations of the chemical potentials induced by a back gate. However the recent discovery of three dimensional semimetals changes the perspective: most of these new semi-metallic materials are stoichiometric and the Fermi-energy is expected to reside at the band crossing. In that situation the transport will be entirely dominated by the physics at the band crossing and will directly probe the topological properties associated with the band crossing points.

Let us put in perspective the association between minimal conductivity and topological properties raised by our results on three band semimetals in two dimensions. In two dimensions, we can extend our analysis for a band crossing described by the simple Hamiltonian $H(\vec{q}) = S_x q_x + S_y q_y$, with S_x, S_y satisfying a spin- S algebra. Again, we find that the Berry topological winding [27] and the minimal conductivity are correlated. In particular for an integer spin S , corresponding to crossing of an odd number of bands, we find that the conductivity vanishes at the crossing, as does the Berry phase [27], while both are finite for half integer spins. In three dimensions, a two band crossing is denoted a Weyl semimetal and is characterized by a

topological Chern number instead of a Berry phase. In that case, the conductance at the nodal point remains finite and scales as $G_{3d} = \ln 2 e^2/(2\pi h)(W/L)^2$ instead of $G_{2d} = e^2/(\pi h)(W/L)$ in two dimensions [28]. Similarly the value of the Fano factor is slightly modified from $F_{2d} = 1/3$ to $F_{3d} \simeq 0.57$. The existence of a finite minimal conductance scaling as $(W/L)^2$ appears to be a robust property associated with the topological two band crossing as its existence is neither modified by a weak disorder [29], nor by an anisotropic deformation of the cone or a tilt of this cone which breaks the local chiral symmetry [30].

METHODS

Topological characterization. The topological characterization of a band crossing point is done by calculating the Berry phase associated to each eigenvector $|\Psi_n\rangle$ upon winding anticlockwise around the crossing point:

$$\gamma_n(\vec{K}) = \frac{-i}{\pi} \oint d\vec{q} \cdot \langle \Psi_n | \vec{\nabla}_{\vec{q}} | \Psi_n \rangle. \quad (10)$$

Conductance and Fano factor. The conductance of a narrow sample is conveniently calculated from the set of the transmission probabilities T_n of the conduction channel labeled by n through the Landauer formula $G = \frac{e^2}{h} \sum_n T_n$. The longitudinal conductivity σ is related to this conductance as $\sigma = LW^{-1}G$. The Fano factor is related to these transmission coefficients as $F = \sum_n T_n(1 - T_n) / \sum_n T_n$. The explicit calculation of the transmission probabilities T_n requires solving the

Schrödinger equation piecewise and matching the solutions at the boundaries of the sample.

Numerical calculations of transport were performed using the Kwant code [31], based on a Green function recursive technique to evaluate the transmission amplitude across a sample. Typical samples of dimensions $L = 100$, $W = 300$ in lattice units were used, using a large po-

tential in the electrodes $eV_\infty W/(v_F \hbar) = 45$, with Fermi velocity $v_F = 3at/(2\hbar)$.

Acknowledgments. We thank F. Piéchon for stimulating discussions about the T_3 model, as well as A. Akhmerov and X. Waintal for helpful advice with the Kwant package. This work was supported by the grants ANR Blanc-2010 IsoTop and ANR Blanc-2012 SemiTopo from the french Agence Nationale de la Recherche.

-
- [1] S. Murakami, *New Journal of Physics* **9**, 356 (2007).
- [2] S. M. Young, S. Zaheer, J. C. Y. Teo, C. L. Kane, E. J. Mele, and A. M. Rappe, *Phys. Rev. Lett.* **108**, 140405 (2012).
- [3] Q. Lv, H. M. Weng, B. B. Fu, X. P. Wang, H. Miao, J. Ma, P. Richard, X. C. Huang, L. X. Zhao, G. F. Chen, Z. Fang, X. Dai, T. Qian, and H. Ding, “Discovery of Weyl semimetal TaAs,” (2015), arXiv:1502.04684.
- [4] S.-Y. Xu, C. Liu, S. K. Kushwaha, R. Sankar, J. W. Krizan, I. Belopolski, M. Neupane, G. Bian, N. Alidoust, T.-R. Chang, H.-T. Jeng, C.-Y. Huang, W.-F. Tsai, H. Lin, P. P. Shibayev, F.-C. Chou, R. J. Cava, and M. Z. Hasan, *Science* **347**, 294 (2015).
- [5] J. Wang, H. Huang, W. Duan, and Z. Liu, *J. Chem Phys* **139**, 184701 (2013).
- [6] W. Li, M. Guo, G. Zhang, and Y.-W. Zhang, *Phys. Rev. B* **89**, 205402 (2014).
- [7] M. Orlita, D. M. Basko, M. S. Zholudev, F. Teppe, W. Knap, V. I. Gavrilenko, N. N. Mikhailov, S. A. Dvoretzkii, P. Neugebauer, C. Faugeras, A.-L. Barra, G. Martinez, and M. Potemski, *Nat Phys* **10**, 233 (2014).
- [8] Z. Wang, Y. Sun, X.-Q. Chen, C. Franchini, G. Xu, H. Weng, X. Dai, and Z. Fang, *Phys. Rev. B* **85**, 195320 (2012).
- [9] Z. K. Liu, B. Zhou, Y. Zhang, Z. J. Wang, H. M. Weng, D. Prabhakaran, S. K. Mo, Z. X. Shen, Z. Fang, X. Dai, Z. Hussain, and Y. L. Chen, *Science* **343**, 864 (2014).
- [10] Z. Wang, H. Weng, Q. Wu, X. Dai, and Z. Fang, *Phys. Rev. B* **88**, 125427 (2013).
- [11] M. Neupane, S.-Y. Xu, R. Sankar, N. Alidoust, G. Bian, C. Liu, I. Belopolski, T.-R. Chang, H.-T. Jeng, H. Lin, A. Bansil, F. Chou, and M. Z. Hasan, *Nature Communications* **5**, 3786 (2014).
- [12] S. Borisenko, Q. Gibson, D. Evtushinsky, V. Zabolotnyy, B. Büchner, and R. J. Cava, *Phys. Rev. Lett.* **113**, 027603 (2014).
- [13] J. A. Steinberg, S. M. Young, S. Zaheer, C. Kane, E. Mele, and A. M. Rappe, *Phys. Rev. Lett.* **112**, 036403 (2014).
- [14] K. S. Novoselov, A. K. Geim, S. V. Morozov, D. Jiang, M. I. Katsnelson, I. V. Grigorieva, S. V. Dubonos, and A. A. Firsov, *Nature* **438**, 197 (2005).
- [15] Y. Zhang, Y.-W. Tan, H. L. Stormer, and P. Kim, *Nature* **438**, 201 (2005).
- [16] J. Tworzydło, B. Trauzettel, M. Titov, A. Rycerz, and C. Beenakker, *Phys. Rev. Lett.* **96**, 246802 (2006).
- [17] M. Katsnelson, *Eur. Phys. J. B* **51**, 157 (2006).
- [18] K. S. Novoselov, E. McCann, S. V. Morozov, V. I. Fal’ko, M. I. Katsnelson, U. Zeitler, D. Jiang, F. Schedin, and A. K. Geim, *Nat Phys* **2**, 177 (2006).
- [19] M. I. Katsnelson, K. S. Novoselov, and A. K. Geim, *Nat Phys* **2**, 620 (2006).
- [20] H. A. Kramers and G. H. Wannier, *Physical Review* **60**, 252 (1941).
- [21] A. Raoux, M. Morigi, J.-N. Fuchs, F. Piéchon, and G. Montambaux, *Phys. Rev. Lett.* **112**, 026402 (2014).
- [22] F. D. M. Haldane, *Phys. Rev. Lett.* **61**, 2015 (1988).
- [23] W. Hausler, *Phys. Rev. B* **91**, 041102(R) (2015).
- [24] C. W. J. Beenakker, *Rev. Mod. Phys.* **69**, 731 (1997).
- [25] S. Ryu, C. Mudry, A. Furusaki, and A. W. W. Ludwig, *Phys. Rev. B* **75**, 205344 (2007).
- [26] M. Vigh, L. Oroszlány, S. Vajna, P. San-Jose, G. Dávid, J. Cserti, and B. Dóra, *Phys. Rev. B* **88**, 161413 (2013).
- [27] B. Dora, J. Kailasvuori, and R. Moessner, *Phys. Rev. B* **84**, 195422 (2011).
- [28] P. Baireuther, J. M. Edge, I. C. Fulga, C. W. J. Beenakker, and J. Tworzydło, *Phys. Rev. B* **89**, 035410 (2014).
- [29] B. Sbierski, G. Pohl, E. J. Bergholtz, and P. W. Brouwer, *Phys. Rev. Lett.* **113**, 026602 (2014).
- [30] M. Trescher, B. Sbierski, P. W. Brouwer, and E. J. Bergholtz, “Quantum transport in dirac materials: signatures of tilted and anisotropic dirac and weyl cones,” (2015), arXiv:1501.04034.
- [31] C. W. Groth, M. Wimmer, A. R. Akhmerov, and X. Waintal, *New Journal of Physics* **16**, 063065 (2014).